

2019

## Eulerian Video Magnification Adaptation for Live Cell Microscopy Analysis

Paul Leamy

*Technological University Dublin, paul.leafy@tudublin.ie*

Jane Courtney

*Technological University Dublin, jane.courtney@tudublin.ie*

Follow this and additional works at: <https://arrow.tudublin.ie/impsfive>

 Part of the [Engineering Commons](#)

---

### Recommended Citation

Leamy, P. & Courtney, J. (2019). Eulerian video magnification adaptation for live cell microscopy analysis. *IMVIP 2019: Irish Machine Vision & Image Processing*, Technological University Dublin, Dublin, Ireland, August 28-30. doi:10.21427/jk1e-t780

This Article is brought to you for free and open access by the IMVIP 2019: Irish Machine Vision and Image Processing at ARROW@TU Dublin. It has been accepted for inclusion in Session 5: Medical and Biomedical Imaging by an authorized administrator of ARROW@TU Dublin. For more information, please contact [arrow.admin@tudublin.ie](mailto:arrow.admin@tudublin.ie), [aisling.coyne@tudublin.ie](mailto:aisling.coyne@tudublin.ie), [vera.kilshaw@tudublin.ie](mailto:vera.kilshaw@tudublin.ie).

# Eulerian Video Magnification Adaptation for Live Cell Microscopy Analysis

Paul Leamy, Jane Courtney

*Biomedical Research Group, Technological University Dublin*

## Abstract

In this paper an adaptation of the Eulerian Video Magnification technique is described for use with .TIFF files produced by a photo-conversion time lapse protocol for live cell microscopy, specifically for research into Acquired Immune Deficiency Syndrome. The tracking and characterisation of a protein found in Human Immunodeficiency Virus, to determine its dynamics and pathways is a key determinant in understanding the protein's function. The aim of this algorithm is to process an image sequence in the temporal direction with the result being that changes in fluorescence for particular pixel locations, or regions of interest, are tracked and filtered thereby removing noise which is inherent with these types of images. This reduction in noise produced overall clearer results that will aid in further analysis of the live cells. In addition to this, this implementation attempts to adapt the existing EVM algorithm to aid in the analysis of photo-conversion experiments. The algorithm will decompose images into a multi-scale representation, and filter images in the temporal domain, recompose the image with amplifications applied to exaggerate particular motions in the images sequence. This paper also investigates the applicability of this magnification, to determine if it is practical in the situation of tracking protein dynamics. Modification of captured data is to be kept at a minimum to reduce the possibility of misinterpretation of the data.

**Keywords:** Eulerian, Video, Magnification, Protein, Tracking

## 1 Introduction

Photo-conversion (PC) experiments consist of defining a Region of Interest (ROI) in which biologists are able to selectively label sub-populations of tagged proteins and to track their sub-cellular migrations in real-time, significantly enhancing the resolution of complex biological processes [Chudakov et al., 2007]. Typical analysis of PC data requires the extraction of fluorescence intensity values within the ROIs, widely handled by commercial microscope software control packages in conjunction with the open source project, ImageJ [Abràmoff et al., 2004]. The evolution of pixel intensities over the entire image sequence can be used to classify different ROIs in the images of these cells. These experiments work by injecting cells with a protein that becomes fluorescent under particular lighting conditions and the spreading of the protein is tracked over time. The area of the cell can either be classed as Accumulation, Migration (towards), Migration (Away) or unclassified depending upon the trend that the fluorescence takes.

Shown in Figure 1 is a typical plot of fluorescence from the photo conversion experiment. It can be seen that the gradual motions that are of interest can be of a low amplitude overall and even corrupted by noise

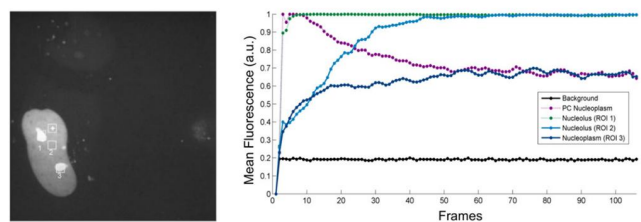


Figure 1: Highlighted in this figure are 5 key regions of interest and corresponding time-series representations of fluorescence produced by a photo-conversion time lapse protocol for live cell microscopy for research into AIDS.

introduced during the image capturing process. Using the Eulerian Video Magnification (EVM) technique outlined below, the gradual motions seen in the image sequence will be isolated using Laplacian Pyramids and temporal filtering and then amplified. At the same time noise present in the image sequences will be reduced.

## 2 Eulerian Video Magnification (EVM)

The aim of EVM is to reveal variations in video or image sequences in the temporal/time direction that would be otherwise invisible to the naked eye. The aim of this paper is to adapt the current EVM technique to process the .TIFF image sequences with the goal of amplifying pixel intensities in the temporal direction in Regions of Interest (ROI) while suppressing unwanted features such as noise.

The EVM technique comes from research in Massachusetts Institute of Technology (MIT) [Wu et al., 2012]. The drive behind this project came from the idea that all video sequences, although they may seem static, contain changes that are so slight that the human eye may be unable to detect them. The goal of EVM is to make these subtle changes visible or better yet provide a way to visualize these changes by means of isolating the desired or signals of interest and amplifying them accordingly to make them more prominent within the processed video sequences.

Some examples of what this has been used for includes medical applications [Li et al., 2018], mechanical applications [Wadhwa et al., 2016] as well as gaming and entertainment applications. Variations in image intensities in video frames can be isolated and exaggerated to show up more clearly after processing. One example for medical applications is that the colour variations in human skin. By isolating the red channel at frequencies similar to the human heart rate blood flow in the skin can be seen. This can be used to help in the diagnosis of numerous conditions related to heart and circulation problems.

The code for this program has been developed from the beginning using MIT's research [Wu et al., 2012] as a starting point and is not a direct implementation of their own code. To implement the EVM algorithm, the following steps are to be executed.

- Step 1 - A Laplacian Pyramid using of each frame in the image sequence is constructed. This produces a multi-scale representation of the original image sequence where each level of the Laplacian pyramid is a band-passed version of the original image.
- Step 2 - The time series (temporal direction) data corresponding to the value a pixel on each level of the Laplacian pyramid is filtered to extract frequencies of interests. Filter specification depends upon the application.
- Step 3 - Extracted filtered signals are amplified/attenuated by an “*alpha*” factor (referred to as an  $\alpha$ -factor from here on), and added to the pre-filtered image sequence.
- Step 4 - The pyramid levels of the the combined images are then collapsed back into a single image sequence to generate the output image sequence.

This process is illustrated in Figure 2 with an example of the EVM application from [Wu et al., 2012] included. The significance and procedure for constructing the image pyramids is explained in the next section of this paper.

## 3 Image Pyramids

Image Pyramids are used as a means of hierarchical image representation, which were developed to decompose images into information at multiple scales. These image pyramids can be used to extract features that are of interest while also isolating unwanted features such as noise, as the desired information can reside in separate levels of the image pyramids. Image pyramids types include Gaussian, Laplacian [Burt and Adelson, 1983]

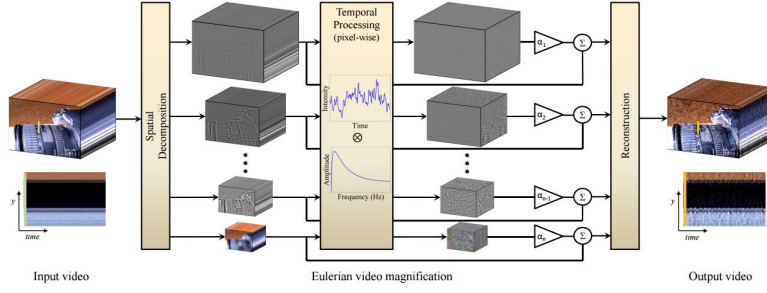


Figure 2: EVM framework and example application [Wu et al., 2012].

and Wavelet [Rockinger, 1997]. For the implementation in this paper only Gaussian and Laplacian pyramids are required.

The Laplacian Pyramid concept is described in the paper by [Burt and Adelson, 1983]. In this paper, Laplacian Pyramids are constructed to be used as means of image encoding and image compression. The levels of the Laplacian Pyramid are band-passed versions of the original image and constructed by finding the difference between adjacent levels of the Gaussian Pyramid. Each level of a Gaussian Pyramid is a consecutively low-passed version of an image. This concept is illustrated in Figure 3.

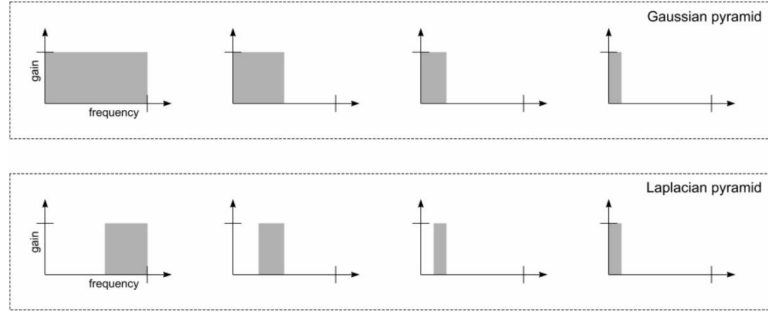


Figure 3: Image Pyramid frequency content at different pyramid levels [Ludwig, 2008]

### 3.1 Gaussian Pyramids

A Gaussian pyramid is a multi-scale representation of an image where each level of the pyramid is a low-pass filtered version of the previous level. To construct the Gaussian pyramid an image undergoes a process called reduction. This is a combination of smoothing (low-pass filtering) and down-sampling. To achieve this an image is convolved with a Gaussian filter kernel  $w(m, n)$ . The reduction function performs both these steps, see (1), where  $l$  is the Gaussian pyramid level and  $m$  and  $n$  are the filter kernel indices and  $i$  and  $j$  are the image coordinates of  $g_l$ .

$$g_l(i, j) = \sum_{m=-2}^2 \sum_{n=-2}^2 w(m, n) g_{l-1}(2i + m, 2j + n) \quad (1)$$

The reverse process of the “reduce” function is also required and this is known as “expand”. The expand function first increases the current level of the Gaussian pyramid image back to the same dimensions as the level previous to its own and interpolates values in between existing pixels again using the same weighting function as the reduce function. An uppercase  $G$  is used to denote an expanded version of a Gaussian pyramid level, see (2),

$$g_{l,n}(i, j) = 4 \sum_{m=-2}^2 \sum_{n=-2}^2 w(m, n) g_{l-1,n}\left(\frac{i-m}{2}, \frac{j-n}{2}\right) \quad (2)$$

### 3.2 Laplacian Pyramids

The Laplacian Pyramid is constructed by computing the difference between adjacent levels of the Gaussian Pyramid. The process of constructing the Laplacian Pyramid can be generalised using the following formula, see (3)

$$L_l = g_l - EXPAND(g_{l-1}) \quad (3)$$

This produces a level of the Laplacian pyramid that is a band-passed section of the original image. The overall Laplacian Pyramid can be viewed as a set of band-pass filtered copies of the original image [Burt and Adelson, 1983]. Each consecutive level of the Laplacian pyramid contains decreasing amounts of fine detail with the lowest level,  $L_0$ , containing the finest amount of detail such as sharp edges.

## 4 Implementation

This implementation of the EVM technique is being carried out in the MATLAB programming environment. Initially, the image sequence is imported into the workspace from a .TIFF file and each frame is stored as the bottom level of the Gaussian pyramid  $g_1$ . At this stage, pre-processing i.e. spatial filtering, contrast stretching and background subtraction of the image sequence can be carried out.

The time series corresponding to pixel values at each level of the Laplacian Pyramid are filtered to extract frequencies of interest. Filters can be designed to suit different applications using different types such as low-pass, Gaussian and band-pass filters with varying pass band and cutoff frequencies. The filtered levels of the Laplacian Pyramid are then amplified with the required  $\alpha$ -factor and added back to the pre-filtered levels of the Laplacian Pyramid. Different  $\alpha$ -factors can be used to amplify or attenuate the influence that each level of the Laplacian Pyramid has on the output image sequence.

All levels of the Laplacian Pyramid are then expanded and added back into each other using the expand function to produce the output image sequence. Pixel intensities in the temporal direction are then compared at common points on the input and output image sequences.

## 5 Testing and Results

### 5.1 Test Conditions and Metrics

Tests 1 through to 4 were carried out to test the effectiveness of the EVM process at reducing temporal noise from the images. For each test, specific  $\alpha$ -factors were used on all images and across all tests the same test points were used. Test 5 is being carried out to display the magnification features associated with EVM technique.

To measure the effectiveness of the filtering and EVM process, the signal-to-noise Ratio (SNR) for the input and output signals is calculated and compared in the tables shown below. To calculate the SNR the inverse of the coefficient of variation  $c_v$  is used. The coefficient of variation is described in (4),

$$c_v = \frac{\sigma}{\mu}, \quad SNR = \frac{1}{c_v} = \frac{\mu}{\sigma}, \quad SNR_{dB} = 20 \log_{10} \left( \frac{\mu}{\sigma} \right) \quad (4)$$

The SNR will give a measure of the ratio of the signal power of the noise power which should increase as the temporal noise is filtered from the image sequence. This will be confirmed in the results section. Four sets of data that are going to be tested are called TT22, TT23, Z19, and Z35.

Each test uses  $\alpha$ -factors which are weighted to each level of the Laplacian Pyramid. Increasing an  $\alpha$ -factor for a particular level will cause that level to have a greater overall influence on the output image. Since the lowest level of the pyramid,  $L_0$ , contains the majority of the spatial noise, this level's influence will be reduced. More gradual motions situated in the higher levels of the pyramid are amplified by applying a higher  $\alpha$ -factor.

## 5.2 Test 1 Results

In test 1, no bias was given to any of the  $\alpha$ -factors. There is a reduction of the amount of noise present in the output images due to the temporal filtering but this is not overly apparent. SNR calculations showed an increase of approximately 5.8dB at all test points on the image sequence.

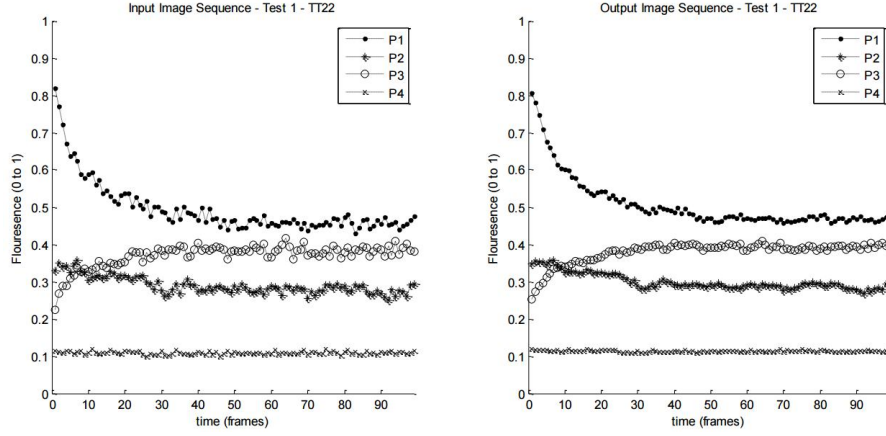


Figure 4: Test 1 input (left) and output (right) fluorescence trends

## 5.3 Test 2 Results

In test 2, the  $\alpha$ -factors associated with the two higher levels of the Laplacian Pyramid were boosted with respect to the other levels. These pyramid levels contain lower frequency information and as a result the amount of noise reduction will increase. This is the case which can be seen visually in Figure 5 and is backed up by the SNR calculations with values ranging from 7.4dB to 7.5dB.

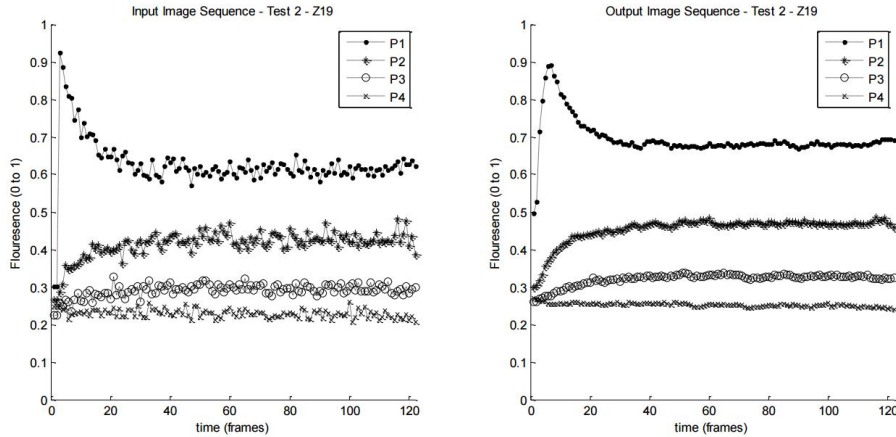


Figure 5: Test 2 input (left) and output (right) fluorescence trends

## 5.4 Test 3 Results

In test 3, there has been a reduction in the amount of noise present but has not been the most effective when compared to the overall test results.

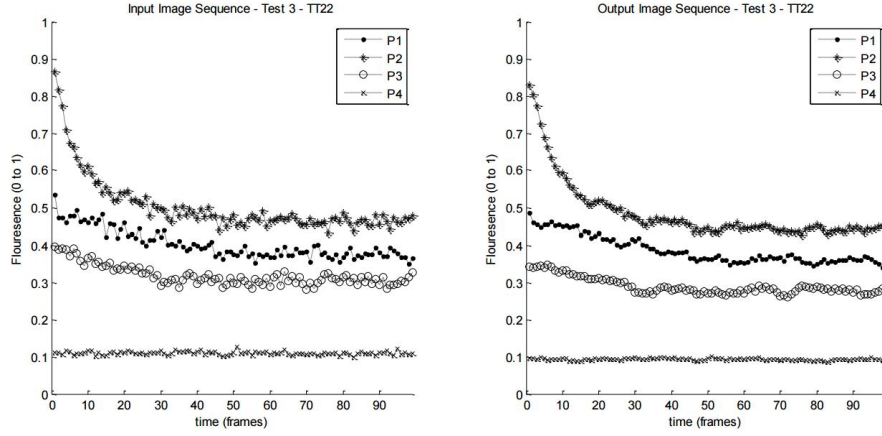


Figure 6: Test 3 input (left) and output (right) fluorescence trends

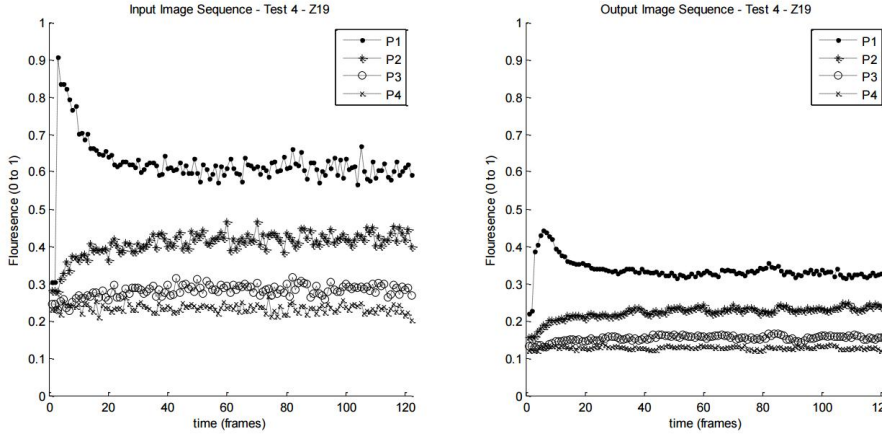


Figure 7: Test 4 input (left) and output (right) fluorescence trends

## 5.5 Test 4 Results

In test 4,  $\alpha$ -factor associated with the lowest levels of the pyramid were boosted. While noise was reduced slightly the trends seen in Figure 7 have become offset and attenuated which is not desirable.

## 5.6 Test 1 - 4 Tabulated Results

Shown in Table 1 is the entire set of results taken from tests 1 through 4 on all sample data used in the experiment. In all cases there has been a reduction in noise, confirmed by the SNR calculations. However, as explained in test 4, it is important that the information contained in the data does not become corrupt using the  $\alpha$ -factors.

Test 2 produced the best results in terms of noise reduction based upon the SNR calculations. This was expected since the higher levels of the Laplacian Pyramid which contain the lower frequency content were amplified during these tests, and in doing so the effects from the noise present on the input sequences has been reduced.

## 5.7 Test 5 Results

In test 5, the effect of using over exaggerated alpha factors is demonstrated. This produces a mixed set of results.

Test Data	Test 1			Test 2			Test 3			Test 4		
TT22	P1	P2	P3	P1	P2	P3	P1	P2	P3	P1	P2	P3
Input $SNR_{dB}$	41.66	36.8	39.06	40.76	36.86	37.94	41.07	37.87	38.53	40.82	36.67	38.23
Output $SNR_{dB}$	47.42	42.67	44.81	48.67	45.13	46.35	44.09	40.6	41.06	44.91	40.4	41.93
TT23												
Input $SNR_{dB}$	36.19	32.66	36.99	36.75	33.02	38.02	36.1	33.39	38.39	33.38	31.5	36.3
Output $SNR_{dB}$	41.96	38.5	42.69	44.53	41.08	45.34	39.53	36.32	42.26	36.05	34.01	39.32
Z19												
Input $SNR_{dB}$	36.23	31.83	29.03	36.39	31.82	28.83	35.66	31.24	27.94	35.85	31.47	28.46
Output $SNR_{dB}$	40.67	36.29	33.48	43.79	39.36	36.37	37.76	33.26	29.99	38.92	34.51	31.47
Z35												
Input $SNR_{dB}$	39.2	40.58	35.89	38.41	40.21	35.5	38.41	39.97	35.2	38.86	40.34	35.52
Output $SNR_{dB}$	45.13	46.4	41.84	47.85	49.22	45.12	43.36	45.1	39.49	41.54	43.26	38.14

Table 1: Table of results for tests 1 through 4. In all of the test scenarios, the use of EVM has resulted in an improvement in signal-to-noise ratio for the images shown in Figure 4 through to Figure 7.

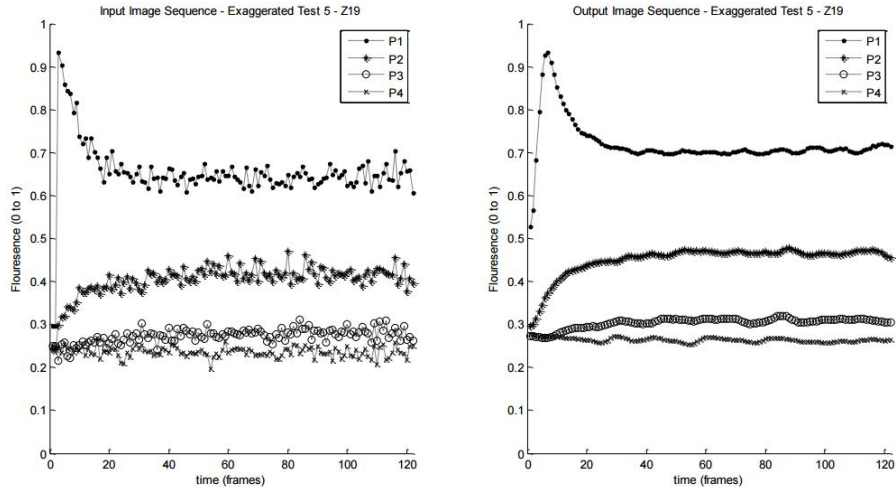


Figure 8: Test 5 Z19 input (left) and output (right) fluorescence trends

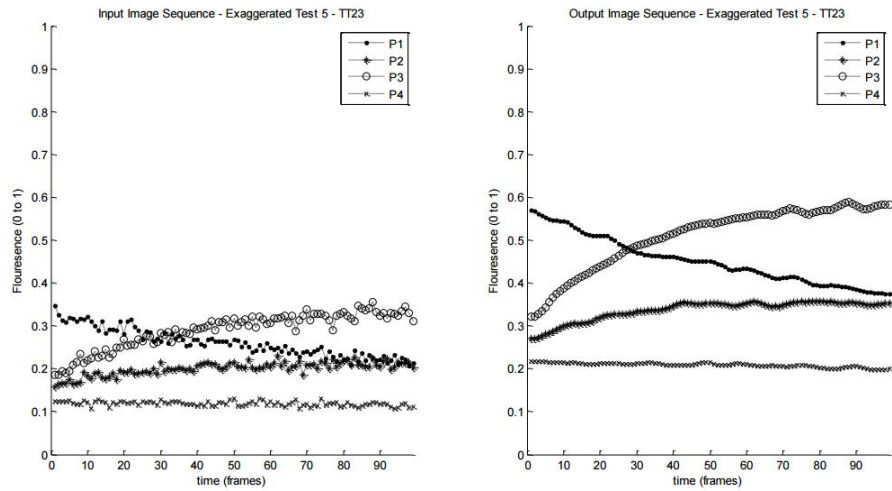


Figure 9: Test 5 TT23 input (left) and output (right) fluorescence trends



In the top two plots of Figure 8 the results show improved noise reduction (SNR increase of 7.2dB) while preserving the general fluorescence trends quite well. In the case of the bottom two trends in Figure 8 there has been noise reduction (SNR increase of 9.4dB) there has also been a very noticeable amount of amplification to all the fluorescence trends.

## 6 Discussion and Conclusions

The SNR measurements combined with the visual inspection of the output data has returned some promising results. An increase in the SNR shows that there has been a reduction in the amount of temporal noise in the image sequences. The introduction of the  $\alpha$ -factors showed that the amount of noise present in the signal compared to the actual signal level can be further decreased. At the time of writing, the  $\alpha$ -factors are experimental and these will require more analysis before a more robust means of calculating an  $\alpha$ -factor is considered. The results look promising and in some cases the amplification that was discussed at the beginning of this paper has been achieved.

It should be noted that this amplification may not be necessarily desirable for when the images undergo analysis at a later stage. The concept that the slower more gradual motions can be amplified and exaggerated has been demonstrated using the  $\alpha$ -factors in the testing section, as was discussed, but care needs to be taken not to render the information useless by altering the original image data too drastically.

Overall, the results would suggest that the aim set out at the start of this project, i.e. to process an image sequence in the temporal direction with the result being that changes in fluorescence for particular pixel locations (ROIs) are tracked and filtered thereby removing noise which is inherent with these types of images using a combination of temporal filtering and EVM, has been achieved.

## References

- [Abràmoff et al., 2004] Abràmoff, M. D., Magalhães, P. J., and Ram, S. J. (2004). Image processing with imagej. *Biophotonics international*, 11(7).
- [Burt and Adelson, 1983] Burt, P. J. and Adelson, E. H. (1983). The laplacian pyramid as a compact image code. *Communications, IEEE Transactions on*, 31(4):532–540.
- [Chudakov et al., 2007] Chudakov, D. M., Lukyanov, S., and Lukyanov, K. A. (2007). Using photoactivatable fluorescent protein dendra2 to track protein movement. *Biotechniques*, 42(5).
- [Li et al., 2018] Li, X., Hong, X., Moilanen, A., Huang, X., Pfister, T., Zhao, G., and Pietikäinen, M. (2018). Towards reading hidden emotions: A comparative study of spontaneous micro-expression spotting and recognition methods. *IEEE Transactions on Affective Computing*, 9(4):563–577.
- [Ludwig, 2008] Ludwig, S. (2008). *Implementation of a spatio-temporal Laplacian image pyramid on the GPU*. PhD thesis, Ph. D. dissertation, Universität zu Lübeck, February.
- [Rockinger, 1997] Rockinger, O. (1997). Image sequence fusion using a shift-invariant wavelet transform. In *Proceedings of international conference on image processing*, volume 3, pages 288–291. IEEE.
- [Wadhwa et al., 2016] Wadhwa, N., Wu, H.-Y., Davis, A., Rubinstein, M., Shih, E., Mysore, G. J., Chen, J. G., Buyukozturk, O., Gutttag, J. V., Freeman, W. T., et al. (2016). Eulerian video magnification and analysis. *Communications of the ACM*, 60(1):87–95.
- [Wu et al., 2012] Wu, H.-Y., Rubinstein, M., Shih, E., Gutttag, J., Durand, F., and Freeman, W. T. (2012). Eulerian video magnification for revealing subtle changes in the world. *ACM Trans. Graph. (Proceedings SIGGRAPH 2012)*, 31(4).